Reflection and transmission coefficients across a fracture

Robiel Martinez Corredor[a)]

Facultad de Ingeniería, Universidad Nacional de La Plata, Calle 1 y 47, La Plata (B1900TAG), Pcia. de Buenos Aires, Argentina.

Juan E. Santos[b)]

CONICET, Instituto del Gas y del Petróleo,Facultad de Ingeniería, Universidad de Buenos Aires, Av. Las Heras 2214 Piso 3, C1127AAR, Buenos Aires, Argentina.

Patricia M. Gauzellino

Departamento de Geofísica Aplicada, Facultad de Ciencias Astronómicas y Geofísicas, Universidad Nacional de La Plata, Paseo del Bosque s/n, La Plata, B1900FWA, Argentina.

José M. Carcione

Istituto Nazionale di Oceanografia e di Geofisica Sperimentale (OGS), Borgo Grotta Gigante 42c, 34010 Sgonico, Trieste, Italy.

[a)]e-mail: robielmartinez@yahoo.com

[b)]Also at Universidad Nacional de La Plata, Calle 1 y 47, La Plata (B1900TAG), Pcia. de Buenos Aires, Argentina and Department of Mathematics, Purdue University, 150 N. University Street, West Lafayette, Indiana, 47907-2067, USA.

Abstract

The numerical modeling is used in many fields of science to explain the behavior of some phenomena understandable. In geophysics, the simulations have application in wave propagation, where the media can be characterized through their seismic responses. Due to the computational cost, the models have to be as simple as possible, reducing the numerical errors that these brings. In this work, we check the approximations (de qu ?) made by Nakagawa and Schoenberg with the exact formulas, because of they simplify the proposed models for media with fractures, characterizing its shear compliance, dry normal compliance and membrane permeability. was the need to

The verification of the proposed models is done by comparing the reflection and transmission coefficients obtained with the answer given by the model of the thin layer (para qu cosa). In examples comparisons are made by varying the permeability and thickness of the fracture; in the last example, three cases of interest were compared; in which the fracture saturated with three different fluids, keeping the background with water.

Contrary to the paper mentioned above, the present paper is devoted to a justified treatment of anisotropic elastic media with one, two, or three systems ...

FIGURAS EN EL PDF ADJUNTO, ESCRIBAN EL ABSTRACT, INTRODUCCION Y CONCLUSIONES, Y DESPUES VEO

SE VERIFICAN LAS APROXIMACIONES DE NAKAGAWA Y SCHOENBERG CON LA FORMULA EXACTA. ESTO ES LO QUE SE HACE. HAY QUE DECIR PORQUE. PORQUE SE VAN A IMPLEMENTAR EN MODELADO NUMERICO? OTRO MOTIVO? HAY QUE SER CONVINCENTE. CUAL ES LA VENTAJA? EN PRINCIPIO SERIA NO USAR CELDAS MUY PEQUENAS, ETC.

I. INTRODUCTION Seismic wave propagation in fractured media is an active area of research, with applications in many fields such us hydrocarbon geophysics exploration, seismic monitoring of reservoir production and mining among others.

Modeling of fractures may be considered as a special case of the thin layer problem, where the fracture is represented by a very thin layer with high permeability and compliance.

There are relatively many works for a layer described by a single-phase (solid) case, e. g., (41) and (2) consider the normal incidence case for a thin layer, (25) studied AVO effects of a thin layer, while the effect of the thickness of a sedimentary layer has been investigated by (17; 18).

(12) computes the scattering response of a lossy layer having orthorhombic symmetry and embedded between two isotropic half-spaces, and (27) obtain the P-wave reflection coefficient in isotropic lossless media as a function of the incidence angle.

Several theories have appeared in the literature to model fractures as boundary conditions in the context of wave propagation phenomena.

The Linear-Slip Interface model (non-welded) for flat viscoelastic two-dimensional fractures was proposed by Schoenberg, (40). This model imposes the continuity of the stresses and discontinuity of the displacements across the fracture.

From laboratory experiences, (20; 21; Pyrak-Nolte et al. 1990) have validated the use of this model. The experiments performed in (20; 21; Pyrak-Nolte et al. 1990) considered the propagation of compressional and shear pulses in dry and wet fractured samples, allowing to validate the seismic discontinuity displacement theory. Also, (28) have assumed thin fractures as an elastic medium very soft in comparison with the frame.(agregar que concluyo)

Concerning wave propagation in fractured fluid-saturated poroelastic media, we mention the boundary conditions given by (**?**). and later by (**?**). In the latter reference, several boundary conditions are developped and the corresponding reflection and transmission coefficients are computed and analyzed. These boundary conditions first consider the most general case in which stresses, velocities and fluid pressure may be discontinuous across a fracture, and later several simplifying hipothesis allow to get other forms of the boundary conditions, one of whjich reduces to that of (**?**).

In numerical simulations, to model fractures as very thin layers would require the use of extremely fine computational meshes, and consequently employing boundary conditions becomes a necessity.

In this paper we determine the frequency range in which the various boundary conditions given in (**?**) are valid to represent fractures in numerical simulation of waves in fractured poroelastic media.

For this purpose, we compare the reflection and transmission coefficients of waves arriving to a plane fracture within a fluid-saturated porous medium represented either as a thin layer or as boundary conditions.

The calculation of the Reflection and Transmission coefficients at a very thin poroelastic separating two poroelastic half-spaces has been perfomed in (**?**). The results were validated againts limiting cases (elastic solid and inviscid fluids and zero layer thickness) and the results predict all wave conversions, critical angles and polarity changes.

To our knowledge, the explicit calculation of the coefficients for poroelastic media has not been addressed. Existing methods are restricted to normal incidence and/or are based on numerical algorithms **(1; 34; 35; 39)**. In general, these works are based on a constitutive equation described by Biot's theory of poroelasticity (5; 6; 13; 14), which is sufficiently general to model the desired characteristics of wave propagation, in particular, the presence of the P waves (type-I and type-II compressional waves) and its effects on interfaces (33**? ? ?**).

There are also jobs where we consider two interfaces, as in (42), where the system is formed by a fluid-saturated porous solid plate inmersed in fluid, and the results are compared with experimental data, and in (22), (?) and (19), where ultrasonic measurements are compared with numerical data in poroelastic slabs.

We solve the scattering problem at all angles of incidence for a single layer embedded between two half-spaces with dissimilar media, where the properties of the media are described by Biot's theory of poroelasticity. The displacement fields are recast in terms of potentials and the boundary conditions at the two interfaces impose continuity of the solid and fluid displacements, normal and shear stresses and fluid pressure. The methodology is analogous to that presented in (37), (36) and Carcione (12; 13), Section 6.4. The results are verified for specific limiting cases with already published theoretical equations (7; 13; 27; 32; 37).

The paper is organized as follows. Biot's theory is reviewed first. Then, we illustrate the methodology and finally we present the examples. The final equations are verified with limiting cases consisting of a single interface in poroelastic media and a layer, where the media can be solids or fluids. The examples are relevant for applications in reflection seismology.

Introduction

For examining the effect of pore fluids,

GUITARRA. LA INTRODUCCION CONSISTE EN REVIEW, CLAIM Y LO QUE SE HACE EN EL PAPER, 3 PARAGRAFOS

II. BIOT'S THEORY

We consider a porous solid saturated by a viscous compressible fluid and assume that the whole aggregate is isotropic. Let U and U_f be the averaged displacement vectors of the solid and fluid parts of the medium, respectively. Then, W is defined as the averaged relative fluid displacement per unit volume of bulk material,

$$W = \phi \left(U_f - U \right), \tag{1}$$

where ϕ is the effective porosity.

Let ε_{ij} and σ_{ij} denote the strain tensors of the solid and the bulk material, respectively, and let P_f denote the fluid pressure. Following (5; 6), the stress-strain relations can be written as

$$\begin{aligned} \sigma_{ij} &= 2\mu\varepsilon_{ij}(U) + \delta_{ij} \left(\lambda_c \nabla\cdot U + D\nabla\cdot W \right), \quad i,j = 1,2,3, \\ P_f &= -D\nabla\cdot U - M\nabla\cdot W \end{aligned} \tag{2}$$

(13). Here, μ is the wet-rock shear modulus of the bulk material, considered to be equal to the shear modulus of the dry-rock. The grains are characterized by density ρ_s, bulk modulus K_s and shear modulus μ_s, while the fluid by ρ_f, K_f, and viscosity η. The grains are assumed to form an elastic porous matrix characterized by a porosity ϕ, permeability κ, bulk modulus K_m, and shear modulus μ_m. The Lamé constants of the saturated rock are λ_c and μ. The constants λ_c, D and M in (2) can be written as (13)

$$\alpha = 1 - \frac{K_m}{K_s}, \quad M = \left(\frac{\alpha - \phi}{K_s} + \frac{\phi}{K_f} \right)^{-1}, \quad D = \alpha\ M,$$
$$K_c = K_m + \alpha^2 M, \quad \lambda_c = K_c - \frac{2}{3}\mu, \quad BK_u = D,$$
$$B = \frac{1/K_m - 1/Ks}{1/K_m - 1/K_s + \phi(1/K_f - 1/K_s)}, \tag{3}$$

where K_u is the undrained bulk modulus.

Next, let

$$\rho_b = (1 - \phi)\,\rho_s + \phi \rho_f \tag{4}$$

be the mass density of the bulk material. Also, let g and b denote the mass and viscous coupling coefficients between the solid and fluid phases (3; 4):

$$g = \frac{S\rho_f}{\phi}, \quad b = \frac{\eta}{\kappa}, \quad S = \frac{1}{2}\left(1 + \frac{1}{\phi}\right), \tag{5}$$

where S is known as the structure factor. If g and b are functions of frequency, we have

$$b(\omega) = \mathrm{Re}\left(\frac{\eta}{\kappa(\omega)}\right),$$
$$g(\omega) = \frac{1}{\omega}\mathrm{Im}\left(\frac{\eta}{\kappa(\omega)}\right), \tag{6}$$

being $\kappa(\omega)$ the dynamic permeability, a complex function defined in (23), and given by

$$\kappa(\omega) = \kappa_0 \left(\sqrt{1 + \mathrm{i}\frac{4\omega}{n_j \omega_j}} + \mathrm{i}\frac{\omega}{\omega_j} \right)^{-1}, \tag{7}$$

where κ_0 is the absolute permeability, n_j is a finite parameter determined by the pore geometry and ω_j is the viscous-boundary characteristic frequency given by $\omega_j = \eta\phi/(\kappa_0 \rho_f S)$ (13; 23).

Then, assuming constant coefficients μ, λ_c, D, and M in (2), Biot's equations of motion can be stated as (5; 6; 13)

$$\begin{aligned}
\nabla\cdot \sigma &= H_c \nabla\left(\nabla\cdot U\right) - \mu\nabla\times\left(\nabla\times U\right) + D\nabla\left(\nabla\cdot W\right) \\
&= \rho_b \frac{\partial^2 U}{\partial t^2} + \rho_f \frac{\partial^2 W}{\partial t^2}, \\
-\nabla P_f &= D\nabla\left(\nabla\cdot U\right) + M\nabla\left(\nabla\cdot W\right) \\
&= \rho_f \frac{\partial^2 U}{\partial t^2} + g\frac{\partial^2 W}{\partial t^2} + b\frac{\partial W}{\partial t},
\end{aligned} \tag{8}$$

where $H_c = \lambda_c + 2\mu$.

A plane-wave analysis shows that in this type of media two compressional waves (type-I and type-II waves) and one shear of S-wave can propagate (5).

III. REFLECTION AND TRANSMISSION COEFFICIENTS OF A SINGLE LAYER

The fluid-saturated system consists of three media, $\Omega_n,\ n = 1, 2, 3$ with different properties as shown in Figure 1. Let $z = 0$ be the boundary between Ω_1 and Ω_2, and $z = h$ the boundary between Ω_2 and Ω_3, and consider a type-I compressional plane wave in Ω_1 incident at $z = 0$ with an angle θ_{i1} with respect to the vertical z-axis. Following (38), we represent the incident, reflected and transmitted waves using potentials.

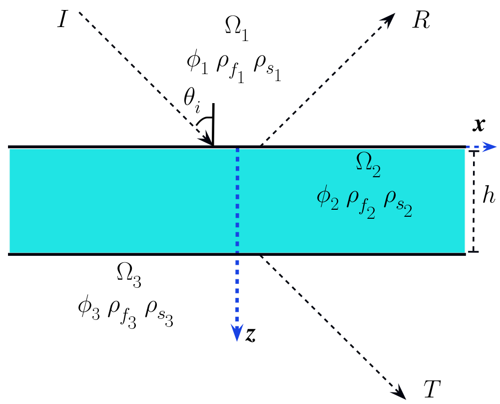

Figure 1: Geometry of the two half-spaces and the embedded layer.

For Ω_1 the potentials of the solid and relative fluid displacement are given by

$$\begin{aligned} \varphi_{i1} &= A_{i1} e^{\mathrm{i}(\omega t - \mathbf{q}_{i1}\cdot\mathbf{x})}, \\ \psi_{i1} &= B_{i1} e^{\mathrm{i}(\omega t - \mathbf{q}_{i1}\cdot\mathbf{x})}, \end{aligned} \tag{9}$$

where

$$\mathbf{q}_{i1} = q_{i1}\left(\sin(\theta_{i1}), \cos(\theta_{i1})\right),$$

is the complex wave vector determining the polarization direction.

Let $\varphi_{rc}^{(1)}$, $\varphi_{rs}^{(1)}$, $\psi_{rc}^{(1)}$ and $\psi_{rs}^{(1)}$ be the compressional and shear potentials of the solid and relative fluid displacement, for the reflected waves in Ω_1. They are given by

$$\begin{aligned}
\varphi_{rc}^{(1)} &= A_{r1}^{(1)} e^{\mathrm{i}(\omega t - \mathbf{q}_{r1}^{(1)}\cdot\mathbf{x})} + A_{r2}^{(1)} e^{\mathrm{i}(\omega t - \mathbf{q}_{r2}^{(1)}\cdot\mathbf{x})}, \\
\varphi_{rs}^{(1)} &= A_{rs}^{(1)} e^{\mathrm{i}(\omega t - \mathbf{q}_{rs}^{(1)}\cdot\mathbf{x})}, \\
\psi_{rc}^{(1)} &= B_{r1}^{(1)} e^{\mathrm{i}(\omega t - \mathbf{q}_{r1}^{(1)}\cdot\mathbf{x})} + B_{r2}^{(1)} e^{\mathrm{i}(\omega t - \mathbf{q}_{r2}^{(1)}\cdot\mathbf{x})}, \\
\psi_{rs}^{(1)} &= B_{rs}^{(1)} e^{\mathrm{i}(\omega t - \mathbf{q}_{rs}^{(1)}\cdot\mathbf{x})},
\end{aligned} \tag{10}$$

where the subscript r indicates the reflected wave, c indicates compressional wave and s shear wave, the super-index (1) refers to medium 1. Subscripts 1 and 2 indicate type-I and type-II waves, respectively.

In Ω_2, the potentials are

$$\begin{aligned}
\varphi_{tc}^{(2)} &= A_{t1}^{(2)} e^{\mathrm{i}(\omega t - \mathbf{q}_{t1}^{(2)}\cdot\mathbf{x})} + A_{t2}^{(2)} e^{\mathrm{i}(\omega t - \mathbf{q}_{t2}^{(2)}\cdot\mathbf{x})}, \\
\varphi_{ts}^{(2)} &= A_{ts}^{(2)} e^{\mathrm{i}(\omega t - \mathbf{q}_{ts}^{(2)}\cdot\mathbf{x})}, \\
\psi_{tc}^{(2)} &= B_{t1}^{(2)} e^{\mathrm{i}(\omega t - \mathbf{q}_{t1}^{(2)}\cdot\mathbf{x})} + B_{t2}^{(2)} e^{\mathrm{i}(\omega t - \mathbf{q}_{t2}^{(2)}\cdot\mathbf{x})}, \\
\psi_{ts}^{(2)} &= B_{ts}^{(2)} e^{\mathrm{i}(\omega t - \mathbf{q}_{ts}^{(2)}\cdot\mathbf{x})}, \\
\varphi_{rc}^{(2)} &= A_{r1}^{(2)} e^{\mathrm{i}(\omega t - \mathbf{q}_{r1}^{(2)}\cdot\mathbf{x})} + A_{r2}^{(2)} e^{\mathrm{i}(\omega t - \mathbf{q}_{r2}^{(2)}\cdot\mathbf{x})}, \\
\varphi_{rs}^{(2)} &= A_{rs}^{(2)} e^{\mathrm{i}(\omega t - \mathbf{q}_{rs}^{(2)}\cdot\mathbf{x})}, \\
\psi_{rc}^{(2)} &= B_{r1}^{(2)} e^{\mathrm{i}(\omega t - \mathbf{q}_{r1}^{(2)}\cdot\mathbf{x})} + B_{r2}^{(2)} e^{\mathrm{i}(\omega t - \mathbf{q}_{r2}^{(2)}\cdot\mathbf{x})}, \\
\psi_{rs}^{(2)} &= B_{rs}^{(2)} e^{\mathrm{i}(\omega t - \mathbf{q}_{rs}^{(2)}\cdot\mathbf{x})}
\end{aligned} \tag{11}$$

and the subscript t indicates the transmitted wave.

Finally, potentials in Ω_3 are expressed by

$$
\begin{aligned}
\varphi_{tc}^{(3)} &= A_{t1}^{(3)} e^{\mathrm{i}(\omega t-\mathbf{q}_{t1}^{(3)}\cdot\mathbf{x})} + A_{t2}^{(3)} e^{\mathrm{i}(\omega t-\mathbf{q}_{t2}^{(3)}\cdot\mathbf{x})},\\
\varphi_{ts}^{(3)} &= A_{ts}^{(3)} e^{\mathrm{i}(\omega t-\mathbf{q}_{ts}^{(3)}\cdot\mathbf{x})},\\
\psi_{tc}^{(3)} &= B_{t1}^{(3)} e^{\mathrm{i}(\omega t-\mathbf{q}_{t1}^{(3)}\cdot\mathbf{x})} + B_{t2}^{(3)} e^{\mathrm{i}(\omega t-\mathbf{q}_{t2}^{(3)}\cdot\mathbf{x})},\\
\psi_{ts}^{(3)} &= B_{ts}^{(3)} e^{\mathrm{i}(\omega t-\mathbf{q}_{ts}^{(3)}\cdot\mathbf{x})}.
\end{aligned}
\tag{12}
$$

In general, we determine $\mathbf{q}_{lj} = (\chi_{lj}, \beta_{lj}) = q_{lj}(\sin(\theta_{lj}), \cos(\theta_{lj}))$, $l = i, r, t$ and $j = 1, 2, s$ for each kind of wave.

The solid and relative fluid vectors $U^{(n)} = \left(U_x^{(n)}, U_z^{(n)}\right)$ and $W^{(n)} = \left(W_x^{(n)}, W_z^{(n)}\right)$ in Ω_n, $n = 1, 2, 3$, are given by (37),

$$
\begin{aligned}
U^{(1)} &= \nabla\varphi_{i1} + \nabla\varphi_{rc}^{(1)} + \left(-\frac{\partial\varphi_{rs}^{(1)}}{\partial z}, \frac{\partial\varphi_{rs}^{(1)}}{\partial x}\right),\\
&= U_{i1}^{(1)} + U_{r1}^{(1)} + U_{r2}^{(1)} + U_{rs}^{(1)}.
\end{aligned}
\tag{13}
$$

$$
\begin{aligned}
W^{(1)} &= \nabla\psi_{i1} + \nabla\psi_{rc}^{(1)} + \left(-\frac{\partial\psi_{rs}^{(1)}}{\partial z}, \frac{\partial\psi_{rs}^{(1)}}{\partial x}\right),\\
&= W_{i1}^{(1)} + W_{r1}^{(1)} + W_{r2}^{(1)} + W_{rs}^{(1)}.
\end{aligned}
\tag{14}
$$

$$
\begin{aligned}
U^{(2)} &= \nabla\varphi_{tc}^{(2)} + \left(-\frac{\partial\varphi_{ts}^{(2)}}{\partial z}, \frac{\partial\varphi_{ts}^{(2)}}{\partial x}\right) + \nabla\varphi_{rc}^{(2)} + \left(-\frac{\partial\varphi_{rs}^{(2)}}{\partial z}, \frac{\partial\varphi_{rs}^{(2)}}{\partial x}\right),\\
&= U_{t1}^{(2)} + U_{t2}^{(2)} + U_{ts}^{(2)} + U_{r1}^{(2)} + U_{r2}^{(2)} + U_{rs}^{(2)}.
\end{aligned}
\tag{15}
$$

$$
\begin{aligned}
W^{(2)} &= \nabla\psi_{tc}^{(2)} + \left(-\frac{\partial\psi_{ts}^{(2)}}{\partial z}, \frac{\partial\psi_{ts}^{(2)}}{\partial x}\right) + \nabla\psi_{rc}^{(2)} + \left(-\frac{\partial\psi_{rs}^{(2)}}{\partial z}, \frac{\partial\psi_{rs}^{(2)}}{\partial x}\right), \\
&= W_{t1}^{(2)} + W_{t2}^{(2)} + W_{ts}^{(2)} + W_{r1}^{(2)} + W_{r2}^{(2)} + W_{rs}^{(2)}.
\end{aligned} \tag{16}
$$

$$
\begin{aligned}
U^{(3)} &= \nabla\varphi_{tc}^{(3)} + \left(-\frac{\partial\varphi_{ts}^{(3)}}{\partial z}, \frac{\partial\varphi_{ts}^{(3)}}{\partial x}\right), \\
&= U_{t1}^{(3)} + U_{t2}^{(3)} + U_{ts}^{(3)}.
\end{aligned} \tag{17}
$$

$$
\begin{aligned}
W^{(3)} &= \nabla\psi_{rc}^{(3)} + \left(-\frac{\partial\psi_{rs}^{(3)}}{\partial z}, \frac{\partial\psi_{rs}^{(3)}}{\partial x}\right), \\
&= W_{t1}^{(3)} + W_{t2}^{(3)} + W_{ts}^{(3)}.
\end{aligned} \tag{18}
$$

Here $U_{lj}^{(n)}$ and $W_{lj}^{(n)}$, $l = i, r, t$, $j = 1, 2, s$, denote the type-I P wave, type-II P wave and shear wave components of $U^{(n)}$ and $W^{(n)}$, respectively. The super-index (n) denotes any variable associated with the medium Ω_n.

The boundary conditions at the interfaces located at $z = 0$ and $z = h$ impose continuity of the solid and fluid displacements, continuity of the normal and shear stress and continuity of the fluid pressure (38). Therefore, at $z = 0$ and $z = h$ we impose the conditions

$$U_x^{(n)} = U_x^{(n+1)}, \tag{19}$$

$$U_z^{(n)} = U_z^{(n+1)}, \tag{20}$$

$$\sigma_{zz}^{(n)} = \sigma_{zz}^{(n+1)}, \tag{21}$$

$$\sigma_{xz}^{(n)} = \sigma_{xz}^{(n+1)}, \tag{22}$$

$$P_f^{(n)} = P_f^{(n+1)}, \tag{23}$$

$$W_z^{(n)} = W_z^{(n+1)}, \quad n = 1, 2. \tag{24}$$

The amplitude of the reflection and transmission coefficients $R_j^{(1)}$ and $T_j^{(3)}$, $j = 1, 2, s$, for the different waves are defined as the ratio of the solid-displacement amplitude of the corresponding wave and that of the incident wave (38), i.e,

$$R_j^{(1)} = \frac{A_{rj}^{(1)} q_{rj}^{(1)}}{A_{i1}^{(1)} q_{i1}^{(1)}}, \tag{25}$$

and

$$T_j^{(3)} = \frac{A_{tj}^{(3)} q_{tj}^{(3)}}{A_{i1}^{(1)} q_{i1}^{(1)}}. \tag{26}$$

Using equations (9)-(12) to obtain expressions for each of the pairs mentioned above and substituting them in (8) leads us to the following relationships between the amplitudes of the solid and the relative amplitudes to the fluid (38):

$$
\begin{aligned}
B_{lj}^{(n)} &= \gamma_{lj}^{(n)} A_{lj}^{(n)}, \quad j=1,2,s, \quad l=r,t, \quad n=1,2,3\ , \\
B_{i1} &= \gamma_{i1} A_{i1},
\end{aligned}
\tag{27}
$$

with

$$
\begin{aligned}
\gamma_{rj}^{(n)} &= \frac{\left[\rho_b^{(n)}\omega^2 - \left(q_{rj}^{(n)}\right)^2 H_c^{(n)}\right]}{\left[\left(q_{rj}^{(n)}\right)^2 D^{(n)} - \rho_f^{(n)}\omega^2\right]} \ \ j=1,2 \ \ n=1,2\ , \\
\gamma_{i1}^{(1)} &= \frac{\left[\rho_b^{(1)}\omega^2 - \left(q_{i1}^{(1)}\right)^2 H_c^{(1)}\right]}{\left[\left(q_{i1}^{(1)}\right)^2 D^{(1)} - \rho_f^{(1)}\omega^2\right]}, \\
\gamma_{tj}^{(n)} &= \frac{\left[\rho_b^{(n)}\omega^2 - \left(q_{tj}^{(n)}\right)^2 H_c^{(n)}\right]}{\left[\left(q_{tj}^{(n)}\right)^2 D^{(n)} - \rho_f^{(n)}\omega^2\right]} \ \ j=1,2 \ \ n=2,3\ , \\
\gamma_{rs}^{(n)} &= \frac{\mu^{(n)}\left(q_{rs}^{(n)}\right)^2 - \rho_b^{(n)}\omega^2}{\rho_f^{(n)}\omega^2} \ \ n=1,2\ , \\
\gamma_{ts}^{(n)} &= \frac{\mu^{(n)}\left(q_{ts}^{(n)}\right)^2 - \rho_b^{(n)}\omega^2}{\rho_f^{(n)}\omega^2} \ \ n=2,3.
\end{aligned}
$$

The boundary conditions (19)-(24) require that the phase factors at the interfaces $z=0$ and $z=h$ are the same:

$$
\begin{aligned}
\chi_{i1} &= \chi_{r1}^{(1)} = \chi_{r2}^{(1)} = \chi_{rs}^{(1)} = \chi_{t1}^{(2)} = \chi_{t2}^{(2)} = \chi_{ts}^{(2)} = \chi_{r1}^{(2)} = \chi_{r2}^{(2)} = \chi_{rs}^{(2)} \\
&= \chi_{t1}^{(3)} = \chi_{t2}^{(3)} = \chi_{ts}^{(3)} = \chi,
\end{aligned}
\tag{28}
$$

which represents Snell's law and allows us to obtain the reflected and transmitted angles θ_{lj} for each type of wave as a function of the incidence angle θ_{i1}.

Application of the boundary conditions (19)-(24) and Snell's law (28) at $z = 0$ and $z = h$ give two systems of linear equations in the unknowns A_{r1} ,A_{r2}, A_{rs}, A_{t1}, A_{t2} and A_{ts} (see Appendix A). These two systems have coefficients depending on the wave numbers $q_{lj}^{(n)}, n = 1, 2, 3, l = i, r, t, j = 1, 2, s$.

Set

$$C_{lj}^{(n)} = A_{lj}^{(n)}/A_{i1}, \quad l = r, t, \quad j = 1, 2, s, \quad n = 1, 2, 3. \tag{29}$$

Using the matrix notation of Carcione (13), Section 6.4 to relate the fields at $z = 0$ and $z = h$ we obtain

$$(\mathbf{A}_1 - \mathbf{B} * \mathbf{A}_3)\, \mathbf{r} = -\mathbf{i}_p, \tag{30}$$

where $\mathbf{r} = \left(C_{r1}^{(1)}, C_{r2}^{(1)}, C_{rs}^{(1)}, C_{t1}^{(3)}, C_{t2}^{(3)}, C_{ts}^{(3)}\right)^{\top}$,
$\mathbf{i}_p = \left[-\chi, -\beta_{i1}^{(1)}, \zeta_{i1}^{(1)}, -2\mu^{(1)}\chi\beta_{i1}^{(1)}, \xi_{i1}^{(1)}, -\beta_{i1}^{(1)}\gamma_{i1}^{(1)}\right]^{\top}$ and $\mathbf{B} = \mathbf{T}(0) * (\mathbf{T}(h))^{-1}$ that acts as a boundary condition. The matrices of the system (30) are given in Appendix B.

The amplitude of the reflection and transmission coefficients for the different types of waves are defined as

$$
\begin{aligned}
R_j^{(1)} &= C_{rj}^{(1)} \frac{q_{rj}^{(1)}}{q_{i1}^{(1)}}, \\
T_j^{(3)} &= C_{tj}^{(3)} \frac{q_{tj}^{(3)}}{q_{i1}^{(1)}}, \quad j = 1, 2, s.
\end{aligned}
\tag{31}
$$

An incident S wave has the same scattering matrix as the P incident wave, but the array $\mathbf{i}_p$ in (30) is replaced by

$$
\mathbf{i}_s = \left[\beta_{is}^{(1)}, -\chi, -\zeta_{is}^{(1)}, -\mu^{(1)} \left\{ \chi^2 - \left(\beta_{is}^{(1)} \right)^2 \right\}, 0, -\gamma_{is}^{(1)} \chi \right]^{\top}.
$$

IV. SEISMIC BOUNDARY CONDITIONS ACROSS A FRACTURE

The model developed by (31) assumes that medium 1 and medium 3 have the same properties and the thickness of medium 2 tends to zero ($h \to 0$). They obtain

$$
\begin{bmatrix}
\dot{U}_x^{(3)} - \dot{U}_x^{(1)} \\
\sigma_{zz}^{(3)} - \sigma_{zz}^{(1)} \\
(-P_f^{(3)}) - (-P_f^{(1)}) \\
\sigma_{xz}^{(3)} - \sigma_{xz}^{(1)} \\
\dot{U}_z^{(3)} - \dot{U}_z^{(1)} \\
\dot{W}_z^{(3)} - \dot{W}_z^{(1)}
\end{bmatrix}
= \frac{\mathrm{i}\omega h}{2}
\begin{bmatrix}
\mathbf{0} & \widetilde{\mathbf{Q}}_{XY} \\
\widetilde{\mathbf{Q}}_{YX} & \mathbf{0}
\end{bmatrix}
\begin{bmatrix}
\dot{U}_x^{(3)} + \dot{U}_x^{(1)} \\
\sigma_{zz}^{(3)} + \sigma_{zz}^{(1)} \\
(-P_f^{(3)}) + (-P_f^{(1)}) \\
\sigma_{xz}^{(3)} + \sigma_{xz}^{(1)} \\
\dot{U}_z^{(3)} + \dot{U}_z^{(1)} \\
\dot{W}_z^{(3)} + \dot{W}_z^{(1)}
\end{bmatrix},
\tag{32}
$$

where the dots over the displacement vector components indicate the time derivate. The matrices $\mathbf{Q}_{XY}$ and $\mathbf{Q}_{YX}$ are given by

$$\widetilde{\mathbf{Q}}_{XY} = \begin{bmatrix} 1/G & \chi/\omega & 0 \\ \chi/\omega & \rho_b^{(2)} & \rho_f^{(2)} \cdot \Pi \\ 0 & \rho_f^{(2)} & \widetilde{\rho}^{(2)} \cdot \Pi \end{bmatrix}, \tag{33}$$

and matrix $\widetilde{\mathbf{Q}}_{YX}$ is gives explicitly as

$$\begin{aligned}
\widetilde{\mathbf{Q}}_{YX}(1,1) &= -4\mu^{(2)}\left(\frac{\chi}{\omega}\right)^2\left(1-\frac{\mu^{(2)}}{H_c^{(2)}}\right)-\frac{\left(\rho_f^{(2)}\right)^2-\rho_b^{(2)}\widetilde{\rho}^{(2)}}{\widetilde{\rho}^{(2)}} \\
&\quad -2\mu^{(2)}\widetilde{B}\widetilde{\beta}\left(\frac{\chi}{\omega}\right)^2\left(-\frac{\rho_f^{(2)}}{\widetilde{\rho}^{(2)}}+\alpha^{(2)}\frac{2\mu^{(2)}}{H_c^{(2)}}\right)\cdot(1-\Pi) \\
\widetilde{\mathbf{Q}}_{YX}(1,2) &= \frac{\chi}{\omega}\left[\left(1-\frac{2\mu^{(2)}}{H_c^{(2)}}\right)+\left(-\frac{\rho_f^{(2)}}{\widetilde{\rho}^{(2)}}+\alpha^{(2)}\frac{2\mu^{(2)}}{H_c^{(2)}}\right)\widetilde{B}\cdot(1-\Pi)\right] \\
\widetilde{\mathbf{Q}}_{YX}(1,3) &= \frac{\chi}{\omega}\left(-\frac{\rho_f^{(2)}}{\widetilde{\rho}^{(2)}}+\alpha^{(2)}\frac{2\mu^{(2)}}{H_c^{(2)}}\right)\cdot\Pi \\
\widetilde{\mathbf{Q}}_{YX}(2,1) &= \frac{\chi}{\omega}\left(1-\frac{2\mu^{(2)}}{H_c^{(2)}}+2\widetilde{B}\widetilde{\beta}\alpha^{(2)}\frac{\mu^{(2)}}{H_c^{(2)}}\cdot(1-\Pi)\right) \\
\widetilde{\mathbf{Q}}_{YX}(2,2) &= \frac{1}{H_c^{(2)}}-\alpha^{(2)}\widetilde{B}\frac{1}{H_c^{(2)}}\cdot(1-\Pi) \\
\widetilde{\mathbf{Q}}_{YX}(2,3) &= -\alpha^{(2)}\frac{1}{H_c^{(2)}}\cdot\Pi \\
\widetilde{\mathbf{Q}}_{YX}(3,1) &= \frac{\chi}{\omega}\left[-\frac{\rho_f^{(2)}}{\widetilde{\rho}^{(2)}}+\alpha^{(2)}\frac{2\mu^{(2)}}{H_c^{(2)}}-2\widetilde{B}\widetilde{\beta}\left(\left(\alpha^{(2)}\right)^2\frac{\mu^{(2)}}{H_c^{(2)}}+\frac{\mu^{(2)}}{M^{(2)}}-\left(\frac{\chi}{\omega}\right)^2\frac{\mu^{(2)}}{\widetilde{\rho}^{(2)}}\right)\cdot(1-\Pi)\right] \\
\widetilde{\mathbf{Q}}_{YX}(3,2) &= -\alpha^{(2)}\frac{1}{H_c^{(2)}}+\left(\left(\alpha^{(2)}\right)^2\frac{1}{H_c^{(2)}}+\frac{1}{M^{(2)}}-\left(\frac{\chi}{\omega}\right)^2\frac{1}{\widetilde{\rho}^{(2)}}\right)\widetilde{B}\cdot(1-\Pi) \\
\widetilde{\mathbf{Q}}_{YX}(3,3) &= \left(\left(\alpha^{(2)}\right)^2\frac{1}{H_c^{(2)}}+\frac{1}{M^{(2)}}-\left(\frac{\chi}{\omega}\right)^2\frac{1}{\widetilde{\rho}^{(2)}}\right)\cdot\Pi,
\end{aligned} \tag{34}$$

where

$$
\begin{aligned}
\widetilde{\rho} &= \mathrm{i}\frac{\eta}{\omega\kappa(\omega)} \\
\frac{1}{\widetilde{B}} &\equiv \alpha^{(2)} + \frac{H_c^{(2)}}{\alpha^{(2)}M^{(2)}} - \left(\frac{\chi}{\omega}\right)^2 \frac{H_c^{(2)}}{\alpha^{(2)}\widetilde{\rho}^{(2)}}, \\
\widetilde{\beta} &\equiv 1 - \frac{H_c^{(2)}\rho_f^{(2)}}{2\alpha^{(2)}\mu^{(2)}\widetilde{\rho}^{(2)}}, \\
\Pi &\equiv \frac{\tanh\epsilon}{\epsilon}, \quad \epsilon \equiv -\frac{\mathrm{i}\beta_{t2}^{(2)}h}{2}.
\end{aligned}
\tag{35}
$$

The properties of medium 2 can be characterized by:

$$\eta_T \equiv \frac{h}{\mu^{(2)}} \quad \text{(shear compliance)}, \tag{36}$$

$$\eta_{N_D} \equiv \frac{h}{H_c^{(2)}} \quad \text{(dry or drained normal compliance)}, \tag{37}$$

$$\widehat{\kappa}(\omega) \equiv \frac{\kappa^{(2)}(\omega)}{h} \quad \text{(membrane permeability)}. \tag{38}$$

Simplifying equation (30), equation (52) of (31) is obtained:

$$
\begin{cases}
\dot{U}_x^{(3)} - \dot{U}_x^{(1)} = (\mathrm{i}\omega)\,\eta_T\sigma_{xz}^{(1)} \\
\dot{U}_z^{(3)} - \dot{U}_z^{(1)} = (\mathrm{i}\omega)\,\eta_{N_D}\left[\left(1-\alpha^{(2)}\widetilde{B}\,(1-\Pi)\right)\sigma_{zz}^{(1)} - \alpha^{(2)}\frac{-P_f^{(3)}+\left(-P_f^{(1)}\right)}{2}\cdot\Pi\right] \\
\dot{W}_z^{(3)} - \dot{W}_z^{(1)} = (\mathrm{i}\omega)\,\alpha^{(2)}\eta_{N_D}\left[-\sigma_{zz}^{(1)} + \frac{1}{\widetilde{B}}\frac{-P_f^{(3)}+\left(-P_f^{(1)}\right)}{2}\right]\cdot\Pi \\
\sigma_{xz}^{(3)} = \sigma_{xz}^{(1)} \\
\sigma_{zz}^{(3)} = \sigma_{zz}^{(1)} \\
-P_f^{(3)} - \left(-P_f^{(1)}\right) = \frac{\eta_f^{(2)}}{\widehat{\kappa}(\omega)}\frac{\dot{W}_z^{(3)}+\dot{W}_z^{(1)}}{2}\cdot\Pi
\end{cases}
\tag{39}
$$

where $\widetilde{\beta} \approx 1$ and

$$\widetilde{B} = \alpha^{(2)} \frac{M^{(2)}}{H_u^{(2)}},$$
$$H_u^{(2)} = K_u^{(2)} + \frac{4\mu^{(2)}}{3},$$
$$\epsilon = \frac{1-i}{2}\sqrt{\omega \frac{\alpha^{(2)}\eta_f \eta_{N_D}}{2 * \widetilde{B}\widehat{\kappa}_0}}, \quad \widehat{\kappa}_0 = \kappa_0 / h. \tag{40}$$

When the permeability tends to infinity, equation (53) of (31) is obtained.

$$\begin{cases} \dot{U}_x^{(3)} - \dot{U}_x^{(1)} = (\mathrm{i}\omega)\, \eta_T \sigma_{xz}^{(1)} \\ \dot{U}_z^{(3)} - \dot{U}_z^{(1)} = (\mathrm{i}\omega)\, \eta_{N_D} \left[\sigma_{zz}^{(1)} - \alpha^{(2)} \left(-P_f^{(1)}\right)\right] \\ \dot{W}_z^{(3)} - \dot{W}_z^{(1)} = (\mathrm{i}\omega)\, \alpha^{(2)} \eta_{N_D} \left[-\sigma_{zz}^{(1)} + \frac{1}{\widetilde{B}} \left(-P_f^{(1)}\right)\right] \\ \sigma_{xz}^{(3)} = \sigma_{xz}^{(1)} \\ \sigma_{zz}^{(3)} = \sigma_{zz}^{(1)} \\ -P_f^{(3)} = -P_f^{(1)} \end{cases} \tag{41}$$

V. EXAMPLES

We model the fracture as a thin layer whose reflection coefficient is given by equation (30) assuming h much smaller than the signal wavelength (thin-layer model or TL model). Let us define the fracture-thickness/wavelength ratio, $\mathcal{R}$, where the wavelength is that of the background medium. We consider several cases of interest in reservoir geophysics. Media properties and fracture properties are shown in Table 1 and fluid properties are shown in Table 2. The following cases are taken into account:

Case 1: Comparison between the TL model and equation (30) of (31).

Case 2: Comparison between the TL model and equation (52) of (31).

Case 3: Comparison between the TL model and equation (53) of (31).

Case 4: Calculation of reflection and transmission coefficients for three types of fluid in the fracture, with water in the background medium, using the equation (52) of (31).

A. Case 1

We compute the reflection and transmission coefficients for compressional plane waves propagating through a fracture, where the fluid is water everywhere. Considering the notation in Figure 1, medium 2 is the fracture.

Figure 2 shows the magnitude of the reflection and transmission coefficients for the TL model and equation (30) of (31), where $\mathcal{R} = 3.1 \times 10^{-4}$. When the permeability is very small, there are differences between the two models. In Figure 3, $\mathcal{R} = 3.1 \times 10^{-6}$ and here the coefficients obtained with the two models are the same except at very high frequencies.

B. Case 2

In this case, the TL model is compared with equation (52) of (31). The permeability is $\kappa_0 = 10^{-4}$ D, the incident wave is a type I P-wave and the thickness of the fracture varies from $h = 0.001$ m to $h = 0.00001$ m. When $\mathcal{R} = 3.1 \times 10^{-5}$, at approximately 100 Hz, there are differences between the two models, see Figure 4. But these differences disappear when $\mathcal{R} = 3.1 \times 10^{-7}$.

C. Case 3

In this case, the permeability is infinite ($\kappa_0 \to \infty$). When h =0.001 m and the frequency is 1000 Hz, there are differences in the absolute value of the transmission coefficient obtained with the TL model and equation (53) of (31) when $\mathcal{R} = 3.1 \times 10^{-4}$. If $h = 0.00001$ m there are no differences between the two models. In this case, it is $\mathcal{R} = 3.1 \times 10^{-6}$ for a frequency of 1000 Hz.

D. Case 4

After comparing the present model with that of (31), we proceed to analyze three different cases of interest in reservoir geophysics. The medium is saturated with water and the fracture contains three different fluids, water, oil and gas. The fluid properties are shown in Table 2. The coefficients were calculated for a frequency of 50 Hz and fracture thickness $h = 0.001$ m, which gives $\mathcal{R} = 1.6 \times 10^{-5}$

The reflection and transmission coefficients are calculated with equation (52) of (31) and the results are shown in Figure 6. It can be seen that when the bulk modulus of the fluid in the fracture differs from that of the background, the coefficients vary more. When the fluid density in the fracture is much less than that of the background, the two peaks appearing in the reflection coefficient of the type I wave (R_{PI}) are closer to each other. Also displayed is a peak at 50 degrees in the coefficients of the wave type II (R_{PII} and T_{PII}) when there is gas in the fracture.

VI. CONCLUSIONS

In all cases shown, when the thickness is too small the fracture ratio / wavelength, the results obtained with (31) approximations are similar to the results obtained with the fine layer model, especially for low frequencies . A variable that affects the results very significantly, is the permeability of the fracture; to cases with low permeability fractures, the thickness must be very small, otherwise the approximations and the fine layer model differ, especially at high frequencies. This shows that in certain cases the approximations do not fit the exact model.

In the latter case it is observed that when there is gas in the fracture, the coefficient of reflection of PI-wave, is very different from the other two cases (water or oil in the fracture) and has two lobes between 40 and 60 degrees. Something similar happens with the coefficients of reflection and transmission of shear wave, which appears lobe near 50 degrees only for the case of gas in the fracture. This could be used as an indicator of gas in fractures.

Acknowledgements

This work was partially supported by the Agencia Nacional de Promoción Científica y Tecnológica, Argentina through FONARSEC FSTIC 06/10 and by CONICET from PIP 0952. JMC was partially funded by the CO2Monitor project.

APPENDIX A: LINEAR SYSTEMS

Here, we report the linear equations for the unknown amplitude of the reflected and transmitted waves. First, application of the boundary conditions (19)-(24) at $z = 0$ yields the linear system

$$\begin{aligned} -\chi A_{i1}^{(1)} - \chi A_{r1}^{(1)} - \chi A_{r2}^{(1)} + \beta_{rs}^{(1)} A_{rs}^{(1)} = -\chi A_{t1}^{(2)} - \chi A_{t2}^{(2)} + \beta_{ts}^{(2)} A_{ts}^{(2)} - \chi A_{r1}^{(2)} \\ -\chi A_{r2}^{(2)} + \beta_{rs}^{(2)} A_{rs}^{(2)}. \end{aligned} \tag{A-1}$$

$$\begin{aligned} -\beta_{i1}^{(1)} A_{i1}^{(1)} - \beta_{r1}^{(1)} A_{r1}^{(1)} - \beta_{r2}^{(1)} A_{r2}^{(1)} - \chi A_{rs}^{(1)} = -\beta_{t1}^{(2)} A_{t1}^{(2)} - \beta_{t2}^{(2)} A_{t2}^{(2)} - \chi A_{ts}^{(2)} \\ -\beta_{r1}^{(2)} A_{r1}^{(2)} - \beta_{r2}^{(2)} A_{r2}^{(2)} - \chi A_{rs}^{(2)}. \end{aligned} \tag{A-2}$$

$$\begin{aligned} A_{i1}^{(1)} \zeta_{i1}^{(1)} + A_{r1}^{(1)} \zeta_{r1}^{(1)} + A_{r2}^{(1)} \zeta_{r2}^{(1)} - A_{rs}^{(1)} \zeta_{rs}^{(1)} = A_{t1}^{(2)} \zeta_{t1}^{(2)} + A_{t2}^{(2)} \zeta_{t2}^{(2)} - A_{ts}^{(2)} \zeta_{ts}^{(2)} \\ +A_{r1}^{(2)} \zeta_{r1}^{(2)} + A_{r2}^{(2)} \zeta_{r2}^{(2)} - A_{rs}^{(2)} \zeta_{rs}^{(2)}. \end{aligned} \tag{A-3}$$

$$\begin{aligned} -2\mu^{(1)} A_{i1} \chi \beta_{i1}^{(1)} - 2\mu^{(1)} A_{r1} \chi \beta_{r1}^{(1)} - 2\mu^{(1)} A_{r2} \chi \beta_{r2}^{(1)} - \mu^{(1)} A_{rs} \left[\chi^2 - \left(\beta_{rs}^{(1)} \right)^2 \right] = \\ -2\mu^{(2)} A_{t1} \chi \beta_{t1}^{(2)} - 2\mu^{(2)} A_{t2} \chi \beta_{t2}^{(2)} - \mu^{(2)} A_{ts} \left[\chi^2 - \left(\beta_{ts}^{(2)} \right)^2 \right] - 2\mu^{(2)} A_{r1} \chi \beta_{r1}^{(2)} \\ -2\mu^{(2)} A_{r2} \chi \beta_{r2}^{(2)} - \mu^{(2)} A_{rs} \left[\chi^2 - \left(\beta_{rs}^{(2)} \right)^2 \right]. \end{aligned} \tag{A-4}$$

$$A_{i1}^{(1)}\xi_{i1}^{(1)} + A_{r1}^{(1)}\xi_{r1}^{(1)} + A_{r2}^{(1)}\xi_{r2}^{(1)} = A_{t1}^{(2)}\xi_{t1}^{(2)} + A_{t2}^{(2)}\xi_{t2}^{(2)} + A_{r1}^{(2)}\xi_{r1}^{(2)} + A_{r2}^{(2)}\xi_{r2}^{(2)}. \tag{A-5}$$

$$\begin{aligned} -\beta_{i1}^{(1)}\gamma_2^{(1)}A_{i1}^{(1)} - \beta_{r1}^{(1)}\gamma_1^{(1)}A_{r1}^{(1)} - \beta_{r2}^{(1)}\gamma_2^{(1)}A_{r2}^{(1)} - \chi\gamma_{rs}^{(1)}A_{rs}^{(1)} = -\beta_{t1}^{(2)}\gamma_1^{(2)}A_{t1}^{(2)} \\ -\beta_{t2}^{(2)}\gamma_2^{(2)}A_{t2}^{(2)} - \chi\gamma_{ts}^{(2)}A_{ts}^{(2)} - \beta_{r1}^{(2)}\gamma_1^{(2)}A_{r1}^{(2)} - \beta_{r2}^{(2)}\gamma_2^{(2)}A_{r2}^{(2)} - \chi\gamma_{rs}^{(2)}A_{rs}^{(2)}. \end{aligned} \tag{A-6}$$

Similarly, at $z = h$ we obtain

$$\begin{aligned} -\chi A_{t1}^{(3)}e^{-\mathrm{i}\beta_{t1}^{(3)}h} - \chi A_{t2}^{(3)}e^{-\mathrm{i}\beta_{t2}^{(3)}h} + \beta_{ts}^{(3)}A_{ts}^{(3)}e^{-\mathrm{i}\beta_{ts}^{(3)}h} = -\chi A_{t1}^{(2)}e^{-\mathrm{i}\beta_{t1}^{(2)}h} \\ -\chi A_{t2}^{(2)}e^{-\mathrm{i}\beta_{t2}^{(2)}h} + \beta_{ts}^{(2)}A_{ts}^{(2)}e^{-\mathrm{i}\beta_{ts}^{(2)}h} - \chi A_{r1}^{(2)}e^{-\mathrm{i}\beta_{r1}^{(2)}h} - \chi A_{r2}^{(2)}e^{-\mathrm{i}\beta_{r2}^{(2)}h} \\ +\beta_{rs}^{(2)}A_{rs}^{(2)}e^{-\mathrm{i}\beta_{rs}^{(2)}}. \end{aligned} \tag{A-7}$$

$$\begin{aligned} -\beta_{t1}^{(3)}A_{t1}^{(3)}e^{-\mathrm{i}\beta_{t1}^{(3)}h} - \beta_{t2}^{(3)}A_{t2}^{(3)}e^{-\mathrm{i}\beta_{t2}^{(3)}h} - \chi A_{ts}^{(3)}e^{-\mathrm{i}\beta_{ts}^{(3)}h} = -\beta_{t1}^{(2)}A_{t1}^{(2)}e^{-\mathrm{i}\beta_{t1}^{(2)}h} \\ -\beta_{t2}^{(2)}A_{t2}^{(2)}e^{-\mathrm{i}\beta_{t2}^{(2)}h} - \chi A_{ts}^{(2)}e^{-\mathrm{i}\beta_{ts}^{(2)}h} - \beta_{r1}^{(2)}A_{r1}^{(2)}e^{-\mathrm{i}\beta_{r1}^{(2)}h} - \beta_{r2}^{(2)}A_{r2}^{(2)}e^{-\mathrm{i}\beta_{r2}^{(2)}h} \\ -\chi A_{rs}^{(2)}e^{-\mathrm{i}\beta_{rs}^{(2)}h}. \end{aligned} \tag{A-8}$$

$$\begin{aligned} A_{t1}^{(3)}\zeta_{t1}^{(3)}e^{-\mathrm{i}\beta_{t1}^{(3)}h} + A_{t2}^{(3)}\zeta_{t2}^{(3)}e^{-\mathrm{i}\beta_{t2}^{(3)}h} - A_{ts}^{(3)}\zeta_{ts}^{(3)}e^{-\mathrm{i}\beta_{ts}^{(3)}h} = A_{t1}^{(2)}\zeta_{t1}^{(2)}e^{-\mathrm{i}\beta_{t1}h} \\ +A_{t2}^{(2)}\zeta_{t2}^{(2)}e^{-\mathrm{i}\beta_{t2}^{(2)}h} - A_{ts}^{(2)}\zeta_{ts}^{(2)}e^{-\mathrm{i}\beta_{ts}y} + A_{r1}^{(2)}\zeta_{r1}^{(2)}e^{-\mathrm{i}\beta_{r1}h} + A_{r2}^{(2)}\zeta_{r2}^{(2)}e^{-\mathrm{i}\beta_{r2}h} \\ -A_{rs}^{(2)}\zeta_{rs}^{(2)}e^{-\mathrm{i}\beta_{rs}h}. \end{aligned} \tag{A-9}$$

$$
\begin{aligned}
&-2\mu^{(3)}A_{t1}\chi\beta_{t1}^{(3)}e^{-\mathrm{i}\beta_{t1}^{(3)}h}-2\mu^{(3)}A_{t2}\chi\beta_{t2}^{(3)}e^{-\mathrm{i}\beta_{t2}^{(3)}h}-\mu^{(3)}A_{ts}\left[\chi^2-\left(\beta_{ts}^{(3)}\right)^2\right]e^{-\mathrm{i}\beta_{ts}^{(3)}h}=\\
&-2\mu^{(2)}A_{t1}^{(2)}\chi\beta_{t1}^{(2)}e^{-\mathrm{i}\beta_{t1}^{(2)}h}-2\mu^{(2)}A_{t2}^{(2)}\chi\beta_{t2}^{(2)}e^{-\mathrm{i}\beta_{t2}^{(2)}h}-\mu^{(2)}A_{ts}^{(2)}\left[\chi^2-\left(\beta_{ts}^{(2)}\right)^2\right]e^{-\mathrm{i}\beta_{ts}^{(2)}h}\\
&-2\mu^{(2)}A_{r1}^{(2)}\chi\beta_{r1}^{(2)}e^{-\mathrm{i}\beta_{r1}^{(2)}h}-2\mu^{(2)}A_{r2}^{(2)}\chi\beta_{r2}^{(2)}e^{-\mathrm{i}\beta_{r2}^{(2)}h}-\mu^{(2)}A_{rs}^{(2)}\left[\chi^2-\left(\beta_{rs}^{(2)}\right)^2\right]e^{-\mathrm{i}\beta_{rs}^{(2)}h}.
\end{aligned}
\tag{A-10}
$$

$$
\begin{aligned}
A_{t1}^{(3)}\xi_{t1}^{(3)}e^{-\mathrm{i}\beta_{t1}^{(3)}h}+A_{t2}^{(3)}\xi_{t2}^{(3)}e^{-\mathrm{i}\beta_{t2}^{(3)}h}&=A_{t1}^{(2)}\xi_{t1}^{(2)}e^{-\mathrm{i}\beta_{t1}^{(2)}h}+A_{t2}^{(2)}\xi_{t2}^{(2)}e^{-\mathrm{i}\beta_{t2}^{(2)}h}\\
&+A_{r1}^{(2)}\xi_{r1}^{(2)}e^{-\mathrm{i}\beta_{r1}^{(2)}h}+A_{r2}^{(2)}\xi_{r2}^{(2)}e^{-\mathrm{i}\beta_{r2}^{(2)}h}.
\end{aligned}
\tag{A-11}
$$

$$
\begin{aligned}
&-\beta_{t1}^{(3)}\gamma_1^{(3)}A_{t1}^{(3)}e^{-\mathrm{i}\beta_{t1}^{(3)}h}-\beta_{t2}^{(3)}\gamma_2^{(3)}A_{t2}^{(3)}e^{-\mathrm{i}\beta_{t2}^{(3)}h}-\chi\gamma_{ts}^{(3)}A_{ts}^{(3)}e^{-\mathrm{i}\beta_{ts}^{(3)}h}=\\
&-\beta_{t1}^{(2)}\gamma_1^{(2)}A_{t1}^{(2)}e^{-\mathrm{i}\beta_{t1}^{(2)}h}-\beta_{t2}^{(2)}\gamma_2^{(2)}A_{t2}^{(2)}e^{-\mathrm{i}\beta_{t2}^{(2)}h}-\chi\gamma_{ts}^{(2)}A_{ts}^{(2)}e^{-\mathrm{i}\beta_{ts}^{(2)}h}\\
&-\beta_{r1}^{(2)}\gamma_1^{(2)}A_{r1}^{(2)}e^{-\mathrm{i}\beta_{r1}^{(2)}h}-\beta_{r2}^{(2)}\gamma_2^{(2)}A_{r2}^{(2)}e^{-\mathrm{i}\beta_{r2}^{(2)}h}-\chi\gamma_{rs}^{(2)}A_{rs}^{(2)}e^{-\mathrm{i}\beta_{rs}^{(2)}h}.
\end{aligned}
\tag{A-12}
$$

The coefficients of the systems (A-1)-(A-6) and (A-7)-(A-12) are given by

$$
\begin{aligned}
\beta_{rj}^{(n)} &= -\sqrt{\left(q_{rj}^{(n)}\right)^2-\chi^2}, \quad j=1,2,s \quad n=1,2\ ,\\
\beta_{tj}^{(n)} &= \sqrt{\left(q_{tj}^{(n)}\right)^2-\chi^2}, \quad j=1,2,s \quad n=2,3\ ,\\
\zeta_{lj}^{(n)} &= -\left(q_{lj}^{(n)}\right)^2\left(H_c^{(n)}+D^{(n)}\gamma_{lj}^{(n)}\right)+2\mu^{(n)}\chi^2,\ j=1,2 \quad n=1,2,3 \quad l=i,r,t\ ,\\
\zeta_{ls}^{(n)} &= 2\mu^{(n)}\chi\beta_{ls}^{(n)},\ n=1,2,3 \quad l=r,t\ ,\\
\xi_{lj}^{(n)} &= \left(D^{(n)}+M^{(n)}\gamma_{lj}^{(n)}\right)\left(q_{lj}^{(n)}\right)^2, \quad j=1,2 \quad n=1,2,3 \quad l=i,r,t\ .
\end{aligned}
\tag{A-13}
$$

Now, using equations (3) and (5), we obtain the wave numbers $q_{lj}^{(n)}$, $n = 1, 2, 3$, $l = i, r, t$, and $j = 1, 2, s$:

$$
\begin{aligned}
q_{r1}^{(n)} &= \sqrt{\frac{-F^{(n)} - \sqrt{(F^{(n)})^2 - 4G^{(n)}K^{(n)}}}{2G^{(n)}}}, \quad n = 1, 2, 3\ , \\
q_{r2}^{(n)} &= \sqrt{\frac{-F^{(n)} + \sqrt{(F^{(n)})^2 - 4G^{(n)}K^{(n)}}}{2G^{(n)}}} \quad n = 1, 2, 3\ , \\
q_{rs}^{(n)} &= \sqrt{N^{(n)} - \mathrm{i}V^{(n)}}, \quad n = 1, 2, 3\ , \\
q_{r1}^{(1)} &= q_{i1}^{(1)}, \\
q_{rj}^{(n)} &= q_{tj}^{(n)}, \quad j = 1, 2, s \quad n = 1, 2, 3.
\end{aligned}
\tag{A-14}
$$

Here

$$
\begin{aligned}
G^{(n)} &= M^{(n)}H_c^{(n)} - (D^{(n)})^2, \quad n = 1, 2, 3\ , \\
F^{(n)} &= \omega^2 \left[2\rho_f^{(n)}D^{(n)} - H_c^{(n)}g^{(n)} - \rho_b^{(n)}M^{(n)}\right] + \mathrm{i}H_c^{(n)}b^{(n)}\omega, \quad n = 1, 2, 3\ , \\
K^{(n)} &= \omega^4 \left[\rho_b^{(n)}g^{(n)} - (\rho_f^{(n)})^2\right] - \mathrm{i}\rho_b^{(n)}b^{(n)}\omega^3 \quad n = 1, 2, 3\ , \\
N^{(n)} &= \frac{\omega^2}{\mu^{(n)}}\left[\rho_b^{(n)} - \frac{(\rho_f^{(n)})^2\omega^2 g^{(n)}}{(g^{(n)})^2\omega^2 + (b^{(n)})^2}\right], \quad n = 1, 2, 3\ , \\
V^{(n)} &= (\rho_f^{(n)})^2 \frac{\omega^3 b^{(n)}}{\mu^{(n)}\left((g^{(n)})^2\omega^2 + (b^{(n)})^2\right)}, \quad n = 1, 2, 3\ .
\end{aligned}
$$

APPENDIX B: FINAL SYSTEM OF EQUATIONS

Each of the matrices in the system (30) are defined by

$$\mathbf{A}_1 = \begin{pmatrix} -\chi & -\chi & \beta_{rs}^{(1)} & 0 & 0 & 0 \\ -\beta_{r1}^{(1)} & -\beta_{r2}^{(1)} & -\chi & 0 & 0 & 0 \\ \zeta_{r1}^{(1)} & \zeta_{r2}^{(1)} & -\zeta_{rs}^{(1)} & 0 & 0 & 0 \\ -2\mu^{(1)}\chi\beta_{r1}^{(1)} & -2\mu^{(1)}\chi\beta_{r2}^{(1)} & -\mu^{(1)}\left[\chi^2 - \left(\beta_{rs}^{(1)}\right)^2\right] & 0 & 0 & 0 \\ \xi_{r1}^{(1)} & \xi_{r2}^{(1)} & 0 & 0 & 0 & 0 \\ -\gamma_{r1}^{(1)}\beta_{r1}^{(1)} & -\gamma_{r2}^{(1)}\beta_{r2}^{(1)} & -\gamma_{rs}^{(1)}\chi & 0 & 0 & 0 \end{pmatrix}, \qquad \text{(B-1)}$$

and

$$\mathbf{A}_3 = \left(\begin{matrix} 0 & 0 & 0 \\ 0 & 0 & 0 \\ 0 & 0 & 0 \\ 0 & 0 & 0 \\ 0 & 0 & 0 \\ 0 & 0 & 0 \end{matrix} \right.$$

$$\left.\begin{matrix} -\chi e^{-\mathrm{i}\beta_{t1}^{(3)}h} & -\chi e^{-\mathrm{i}\beta_{t2}^{(3)}h} & \beta_{ts}^{(3)} e^{-\mathrm{i}\beta_{ts}^{(3)}h} \\ -\beta_{t1}^{(3)} e^{-\mathrm{i}\beta_{t1}^{(3)}h} & -\beta_{t2}^{(3)} e^{-\mathrm{i}\beta_{t2}^{(3)}h} & -\chi e^{-\mathrm{i}\beta_{ts}^{(3)}h} \\ \zeta_{t1}^{(3)} e^{-\mathrm{i}\beta_{t1}^{(3)}h} & \zeta_{t2}^{(3)} e^{-\mathrm{i}\beta_{t2}^{(3)}h} & -\zeta_{ts}^{(3)} e^{-\mathrm{i}\beta_{ts}^{(3)}h} \\ -2\mu^{(3)}\chi\beta_{t1}^{(3)} e^{-\mathrm{i}\beta_{t1}^{(3)}h} & -2\mu^{(3)}\chi\beta_{t2}^{(3)} e^{-\mathrm{i}\beta_{t2}^{(3)}h} & -\mu^{(3)}\left[\chi^2 - \left(\beta_{ts}^{(3)}\right)^2\right] e^{-\mathrm{i}\beta_{ts}^{(3)}h} \\ \xi_{t1}^{(3)} e^{-\mathrm{i}\beta_{t1}^{(3)}h} & \xi_{t2}^{(3)} e^{-\mathrm{i}\beta_{t2}^{(3)}h} & 0 \\ -\gamma_{t1}^{(3)}\beta_{t1}^{(3)} e^{-\mathrm{i}\beta_{t1}^{(3)}h} & -\gamma_{t2}^{(3)}\beta_{t2}^{(3)} e^{-\mathrm{i}\beta_{t2}^{(3)}h} & -\gamma_{ts}^{(3)}\chi e^{-\mathrm{i}\beta_{ts}^{(3)}h} \end{matrix}\right). \tag{B-2}$$

Finally, $\mathbf{B} = \mathbf{T}(0) * (\mathbf{T}(h))^{-1}$, and $T(z) = \mathbf{S}_1 * \mathbf{S}_2(z)$, being:

$$\mathbf{S}_1 = \left(\begin{matrix} -\chi & -\chi & \beta_{ts}^{(2)} \\ -\beta_{t1}^{(2)} & -\beta_{t2}^{(2)} & -\chi \\ \zeta_{t1}^{(2)} & \zeta_{t2}^{(2)} & -\zeta_{ts}^{(2)} \\ -2\mu^{(2)}\chi\beta_{t1}^{(2)} & -2\mu^{(2)}\chi\beta_{t2}^{(2)} & -\mu^{(2)}\left[\chi^2 - \left(\beta_{ts}^{(2)}\right)^2\right] \\ \xi_{t1}^{(2)} & \xi_{t2}^{(2)} & 0 \\ -\gamma_{t1}^{(2)}\beta_{t1}^{(2)} & -\gamma_{t2}^{(2)}\beta_{t2}^{(2)} & -\gamma_{ts}^{(2)}\chi \end{matrix}\right.$$

$$
\left.\begin{matrix}
-\chi & -\chi & \beta_{rs}^{(2)} \\
-\beta_{r1}^{(2)} & -\beta_{r2}^{(2)} & -\chi \\
\zeta_{r1}^{(2)} & \zeta_{r2}^{(2)} & -\zeta_{rs}^{(2)} \\
-2\mu^{(2)}\chi\beta_{r1}^{(2)} & -2\mu^{(2)}\chi\beta_{r2}^{(2)} & -\mu^{(2)}\left[\chi^2 - \left(\beta_{rs}^{(2)}\right)^2\right] \\
\xi_{r1}^{(2)} & \xi_{r2}^{(2)} & 0 \\
-\gamma_{r1}^{(2)}\beta_{r1}^{(2)} & -\gamma_{r2}^{(2)}\beta_{r2}^{(2)} & -\gamma_{rs}^{(2)}\chi
\end{matrix}\right), \tag{B-3}
$$

and

$$
\mathbf{S}_2(z) = \begin{pmatrix}
e^{-\mathrm{i}\beta_{t1}^{(2)}z} & 0 & 0 & 0 & 0 & 0 \\
0 & e^{-\mathrm{i}\beta_{t2}^{(2)}z} & 0 & 0 & 0 & 0 \\
0 & 0 & e^{-\mathrm{i}\beta_{ts}^{(2)}z} & 0 & 0 & 0 \\
0 & 0 & 0 & e^{-\mathrm{i}\beta_{r1}^{(2)}z} & 0 & 0 \\
0 & 0 & 0 & 0 & e^{-\mathrm{i}\beta_{r2}^{(2)}z} & 0 \\
0 & 0 & 0 & 0 & 0 & e^{-\mathrm{i}\beta_{rs}^{(2)}z}
\end{pmatrix}. \tag{B-4}
$$

REFERENCES

1. Allard, J. F., Bourdier, R., and Depollier, C. **(1986)**. “Biot waves in layered media,” Journal of Applied Physics, **60**, 1926-1929.

2. Bakke, N. E., and Ursin, B. **(1998)**. “Thin-bed AVO effects,” Geophysical Prospecting, **46**, 571-587.

3. Berryman, J. G. **(1980)**. “Confirmation of Biot’s theory,” Applied Physics Letters, **37**, 382-384.

4. Berryman, J. G. **(1982)**. “Elastic waves in fluid-saturated porous media”. In ”Macroscopic Properties of Disordered Media,” Springer Berlin, Heidelberg, pp. 38-50.

5. Biot, M. A. **(1956)**. “Theory of propagation of elastic waves in a fluid-saturated porous solid. I. Low-frequency range,” The Journal of the Acoustical Society of America, **28**, 168-178.

6. Biot, M. A. **(1962)**. “Mechanics of deformation and acoustic propagation in porous media,” Journal of Applied Physics, **33**, 1482-1498.

7. Brekhovskikh, L. M. **(1980)**. “Waves in layered media,” Academic Press Inc, New York, 2nd edition, pp. 503.

8. Carcione, J. M. **(1996)**. “Elastodynamics of a non-ideal interface: Application to crack and fracture scattering,” Journal of Geophysical Research: Solid Earth, **101**, 28177-28188.

9. Carcione, J. M. **(1997)**. “Reflection and transmission of qP-qS plane waves at a plane boundary between viscoelastic transversely isotropic media,” Geophysical Journal International, **129**, 669-680.

10. Carcione, J. M. **(1998)**. “Scattering of elastic waves by a plane crack of finite width in a transversely isotropic medium,” International Journal for Numerical and Analytical Methods in Geomechanics, **22**, 263-275

11. Carcione, J. M., Gurevich, B., and Cavallini, F. **(2000)**. “A generalized Biot-Gassmann model for the acoustic properties of shaley sandstones,” Geophysical Prospecting, **48**, 539-557.

12. Carcione, J. M. **(2001)**. “Amplitude variations with offset of pressure-seal reflections,” Geophysics, **66**, 283-293.

13. Carcione, J. M. **(2007)**. “Wave fields in real media: Wave propagation in anisotropic, anelastic, porous and electromagnetic media,” Handbook of Geophysical Exploration, vol. 38, Elsevier, Oxford (2nd edition, revised and extended), pp. 538.

14. Carcione, J. M., Morency, C., and Santos, J. E. **(2010)**. “Computational poroelasticity – A review,” Geophysics, **75**, A229-A243.

15. Carcione, J. M., and Picotti, S. **(2012)**. “Reflection and transmission coefficients of a fracture in transversely isotropic media," Studia Geophysica et Geodaetica, **56**, 307-322.

16. Carcione, J. M., Santos, J. E., Ravazzoli, C. L., and Helle, H. B. **(2003)**. "Wave simulation in partially frozen porous media with fractal freezing conditions," Journal of Applied Physics, **94**, 7839-7847.

17. Chung, H. M., and Lawton, D. C. **(1995)**. "Amplitude responses of thin beds: Sinusoidal approximation versus Ricker approximation," Geophysics, **60**, 223-230.

18. Chung, H. M., and Lawton, D. C. **(1996)**. "Frequency characteristics of seismic reflections from thin beds," Canadian Journal of Exploration Geophysics, **31**, 32-37.

19. Fellah, M., Fellah, Z. E. A., Mitri, F. G., Ogam, E., and Depollier, C. **(2013)**. "Transient ultrasound propagation in porous media using Biot theory and fractional calculus : Application to human cancellous bone," The Journal of the Acoustical Society of America, **133**, 1867-1881.

20. Gu B. L., Nihei K. T., Myer L. R. and Pyrak-Nolte L. J. **(1996)**. "Fracture interface waves," Journal of Geophysical Research-Solid Earth, **101**, 827835.

21. Hsu, C. J. and Schoenberg, M. **(1993)**. "Elastic waves through a simulated fractured medium," Geophysics, **58**, 964-977.

22. Johnson, D. L., Plona, T. J., and Kojima, H. **(1994)**. “Probing porous media with first and second sound II. Acoustic properties of water saturated porous media,” Journal of Applied Physics, **76**, 115-125.

23. Johnson, D. L., Koplik, J., and Dashen, R. **(1987)**. “ Theory of dynamic permeability and tortuosity in fluid-saturated porous media,” Journal of fluid mechanics, **176**, 379-402

24. Jocker, J., and Smeulders, D. **(2009)**. “Ultrasonic measurement on poroelastic slabs: Determination of reflection and transmission coefficients and processing for Biot input parameters,” Ultrasonics, **49**, 319-330.

25. Juhlin, C., and Young, R. **(1993)**. “Implication of thin layers for amplitude variation with offset (AVO) studies,” Geophysics, **58**, 1200-1204.

26. Krief, M., Garat, J., Stellingwerff, J., and Ventre, J. **(1990)**. “A petrophysical interpretation using the velocities of P and S waves (full waveform sonic),” The Log Analyst, **31**, 355-369.

27. Liu, L., and Schmitt, D. R. **(2003)**. “Amplitude and AVO responses of a single thin bed,” Geophysics, **68**, 1161-1168.

28. Molotkov, L. A., and Bakulin, A. V. **(1997)**. “An effective model of a fractured medium whit fractures modeled by the surfaces of discontinuity of displacements," Journal of Mathematical Sciences, **86**, 2735-2751.

29. Bakulin, A. V., and Molotkov, L. A. **(1997)**. "Poroelastic medium whit fractures at limiting case of stratified poroelastic medium with thin and soft Biot layers," 67th Annual International Meeting , SEG, Expanded Abstracts, 1001-1004.

30. Molotkov, L. A. **(2004)**. "Wave propagation in anelastic medium intersected by systems of parallel fractures," Journal of Mathematical Sciences, **122**, 3548-3563.

31. Nakagawa, S. and Schoenberg, M. A. **(2007)**. "Poroelastic modeling of seismic boundary conditions across a fracture," The Journal of the Acoustical Society of America, **122**, 831-847.

32. Pilant, W. L. **(1979)**. "Elastic waves in the earth," Elsevier Science Publishing Company, Amsterdam, pp. 493.

Pyrak-Nolte et al. 1990. Pyrak-Nolte, L., Cook, N. G. W., and Myer, L. R., **(1990**]. "Transmission of seismic waves across single natural fractures," J. Geophys. Res., **95**, 8516-8538.

33. Plona, T. **(1980)**. "Observation of a second bulk compressional wave in a porous medium at ultrasonic frequencies," Applied Physics Letters, **36**, 259-261.

34. Pride, S. R., Tromeur, E., and Berryman, J. G. **(2002)**. “Biot slow-wave effects in stratified rock,” Geophysics, **67**, 271-281.

35. Quintal, B., Schmalholz, S.M., and Podladchikov, Y. Y. **(2009)**. “Low-frequency reflections from a thin layer with high attenuation caused by interlayer flow,” Geophysics, **74**, N14-N22.

36. Rubino, J. G., Ravazzoli, C. L., and Santos, J. E. **(2006)**. “Reflection and transmission of waves in composite porous media: A quantification of energy conversions involving slow waves,” The Journal of the Acoustical Society of America, **120**, 2425-2436.

37. Santos, J. E., Corbero, J. M., Ravazzoli, C. L., and Hensley, J. L. **(1992)**. “Reflection and transmission coefficients in fluid-saturated porous media,” The Journal of the Acoustical Society of America, **91**, 1911-1923.

38. Santos, J. E., Ravazzoli, C. L., and Carcione, J. M. **(2004)**. “A model for wave propagation in a composite solid matrix saturated by a single-phase fluid,” The Journal of the Acoustical Society of America, **115**, 2749-2760.

39. Schmidt, H., and Tango, G. **(1986)**. “Efficient global matrix approach to the computation of synthetic seismograms,” Geophysical Journal of the Royal Astronomical Society, **84**, 331-359.

40. Schoenberg, M. **(1980)**. "Elastic wave behavior across linear slip interfaces," J. Acoust Soc. Am., **68**, 1516-1521.

41. Widess, M. B. **(1973)**. "How Thin is a Thin Bed?," Geophysics, **38**, 1176-1180.

42. Wu, K., Xue, Q., and Adler L. **(1990)**. "Reflection and transmission of elastic waves from a fluid-saturated porous solid boundary," The Journal of the Acoustical Society of America, **87**, 2346-2358.

Table 1: Baseline material properties used for the numerical examples are shown.

Properties	Matrix	Fracture
Porosity	0.15	0.5
Solid density (g/m^3)	2.7	2.7
Solid bulk modulus (GPa)	36	36
Frame bulk modulus (GPa)	9	0.0556
Frame shear modulus (GPa)	7	0.0333
Permeability (D)	0.1	100 (case 1, 4)
		0.0001 (case 1)
		0.001 (case 2)
		∞ (case 3)
Tortuosity	3	1

USANDO OTRAS UNIDADES SE SIMPLIFICA. VERIFIQUEN

Table 2: Saturant fluids.

Properties	Gas	Water	Oil
Density (g/m^3)	0.1398	1	0.7
Fluid viscosity (Pa s)	0.000022	0.001	0.004
Fluid bulk modulus (GPa)	0.05543	2.25	0.57

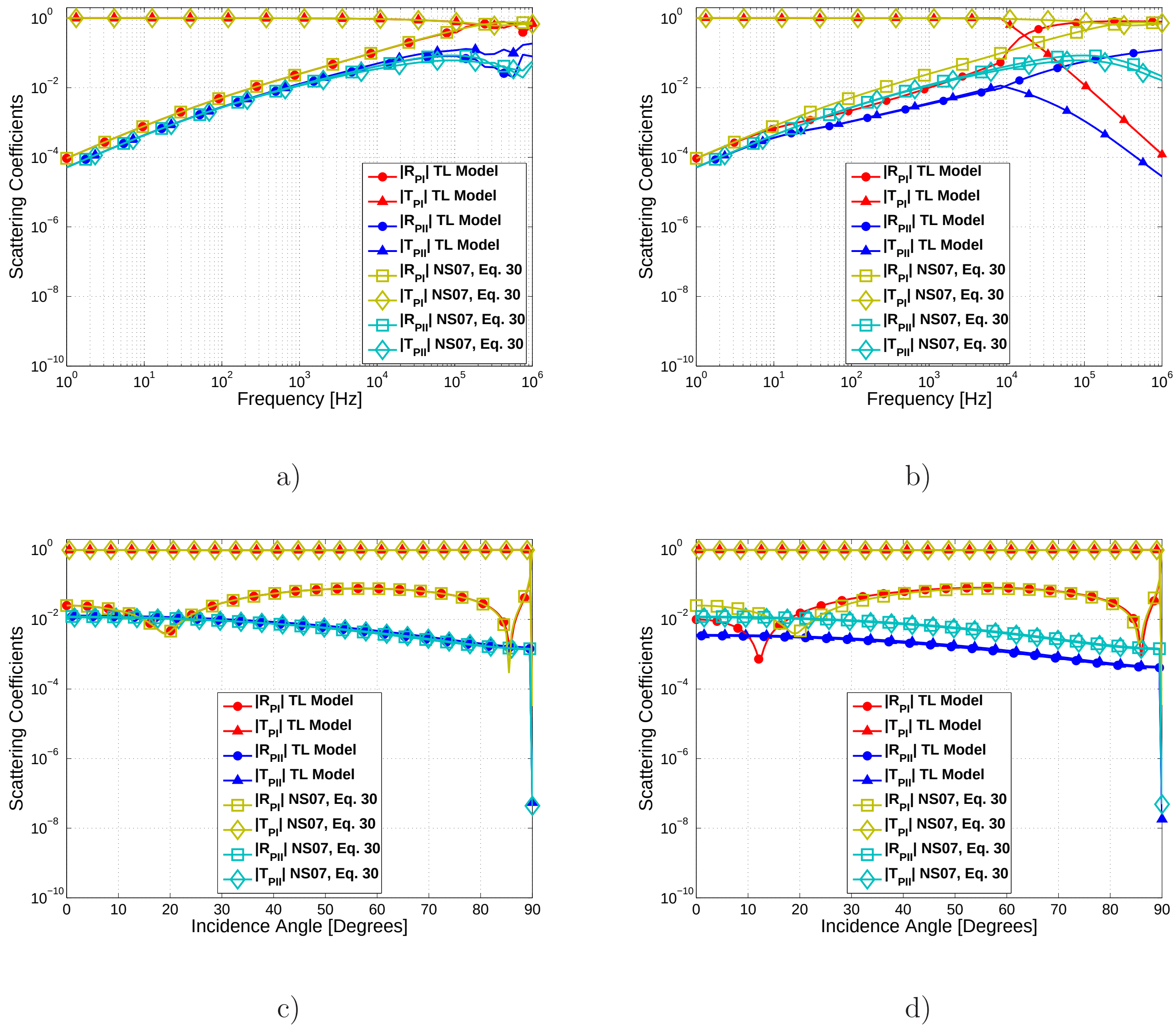

Figure 2: Absolute values of the reflection and transmission coefficients of type I (PI) and type II (PII) P-waves, for two values of permeability. The incident wave is a type I P-wave. The thickness of the fracture is h = 0.001 m. NS07 correspond to (31), and TL model to thin layer model. a) Normal incidence and permeability κ_0 = 100 D b) Normal incidence and permeability κ_0 =0.0001 D. c) Frequency: 1000 Hz and permeability κ_0 = 100 D. d) Frequency: 1000 Hz and permeability κ_0 =0.0001 D.

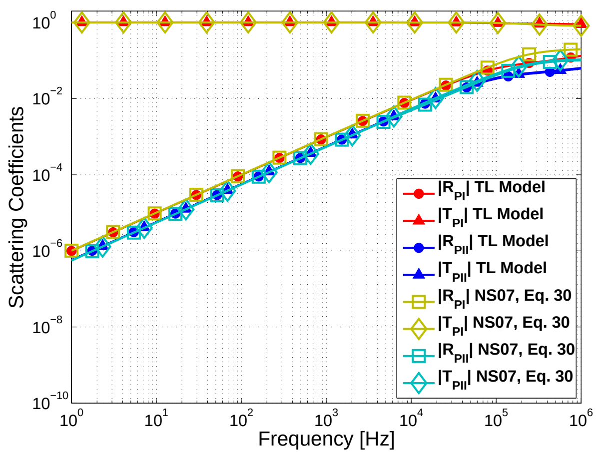

a)

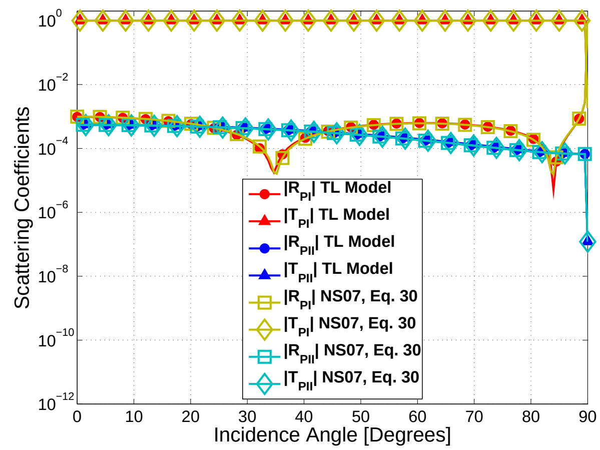

b)

Figure 3: Absolute values of the reflection and transmission coefficients of type I (PI) and type (PII) P-waves. The incident wave is a type I P-wave. The thickness of fracture is $h = 0.00001$ m. NS07 correspond to (31), and TL model to thin layer model a) Normal incidence and permeability $\kappa_0 = 0.0001$ D. b) The frequency is 1000 Hz and the permeability is $\kappa_0 = 0.0001$ D.

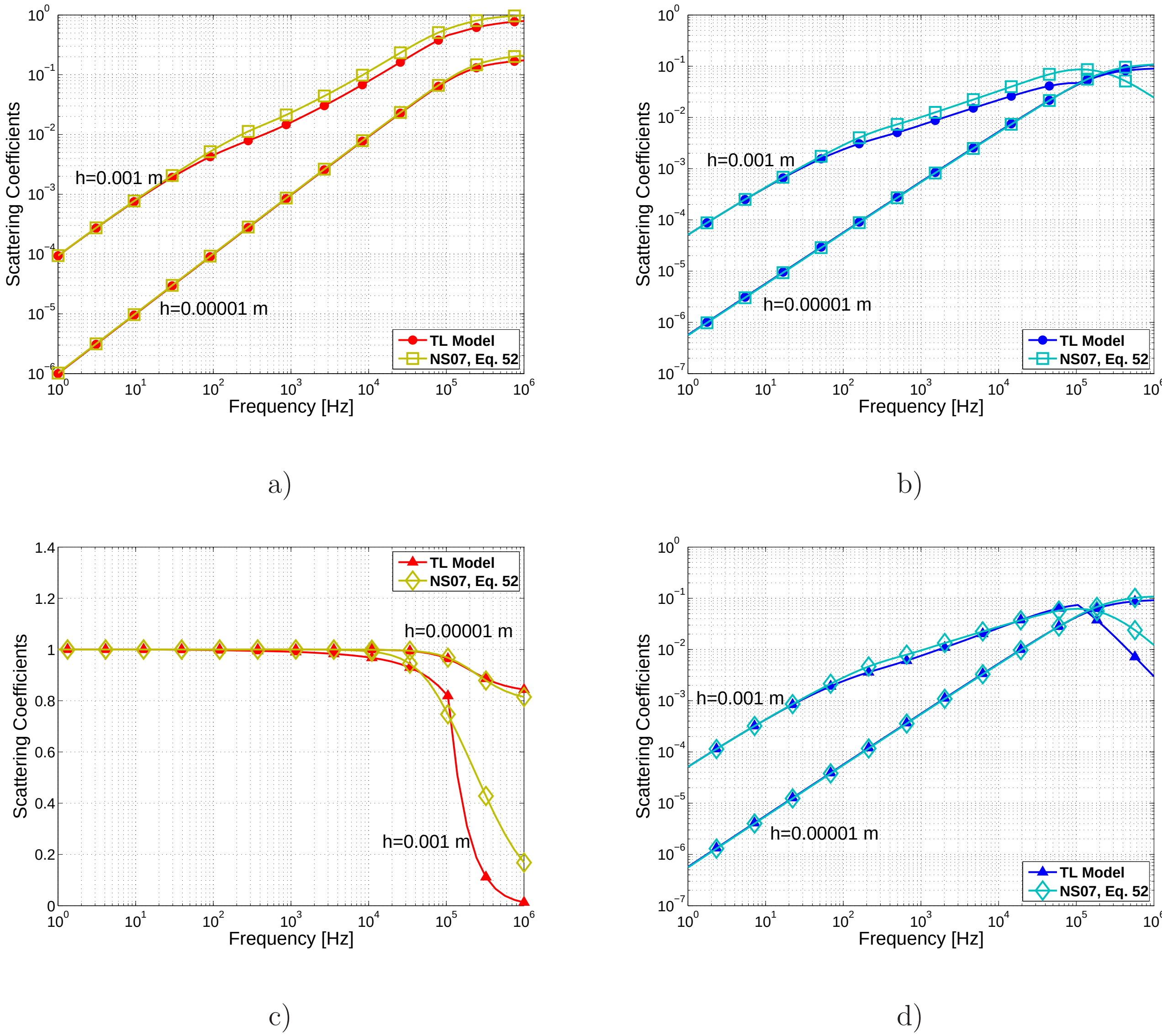

Figure 4: Reflection and transmission coefficients of type I and type II P-waves. The incident wave is a type I P-wave, permeability κ_0 =0.001 D and h varies from 0.001 m to 0.00001 m. NS07 correspond to (31), and TL model to thin layer model. a) Absolute value of the reflection coefficient (type I wave); b) absolute value of the reflection coefficient (type II wave); c) absolute value of the transmission coefficient (type I wave) ; d) absolute value of the transmission coefficient (type I wave).

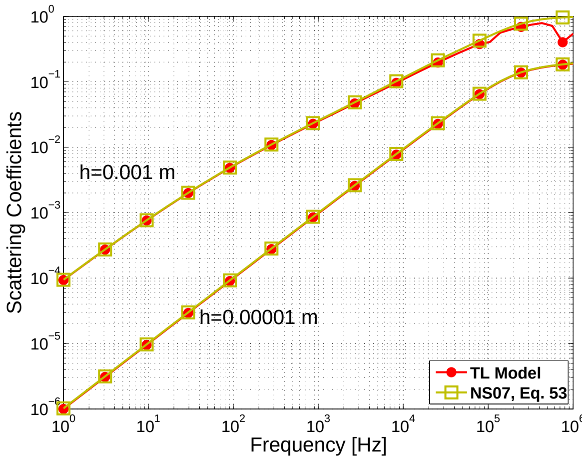

a)

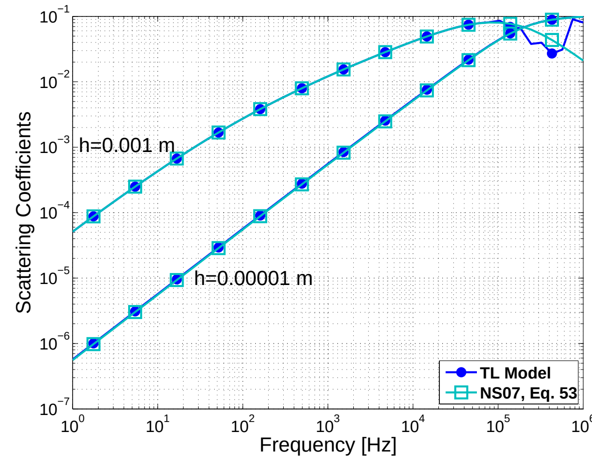

b)

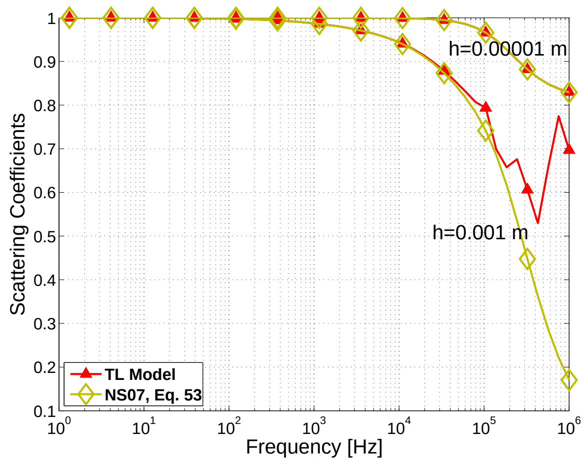

c)

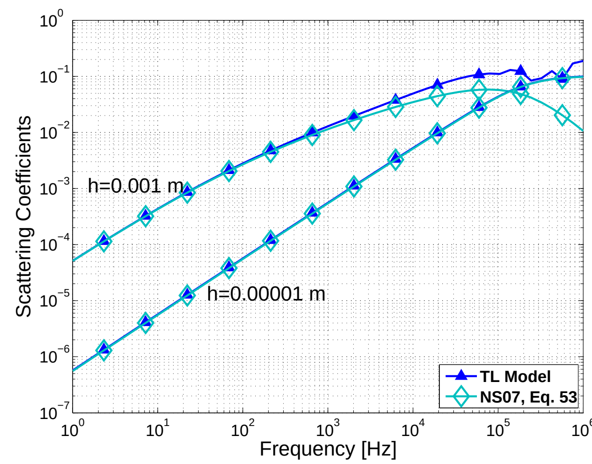

d)

Figure 5: Reflection and transmission coefficients of type I (PI) and type II (PII) P-waves. The incident wave is a type I P-wave, permeability $\kappa_0 \to \infty$ and h varies from 0.001 m to 0.00001 m. NS07 correspond to (31), and TL model to thin layer model. a) Absolute value of the reflection coefficient (type I wave); b) absolute value of the reflection coefficient (type II wave); c) absolute value of the transmission coefficient (type I wave); e) absolute value of the transmission coefficient (type I wave).

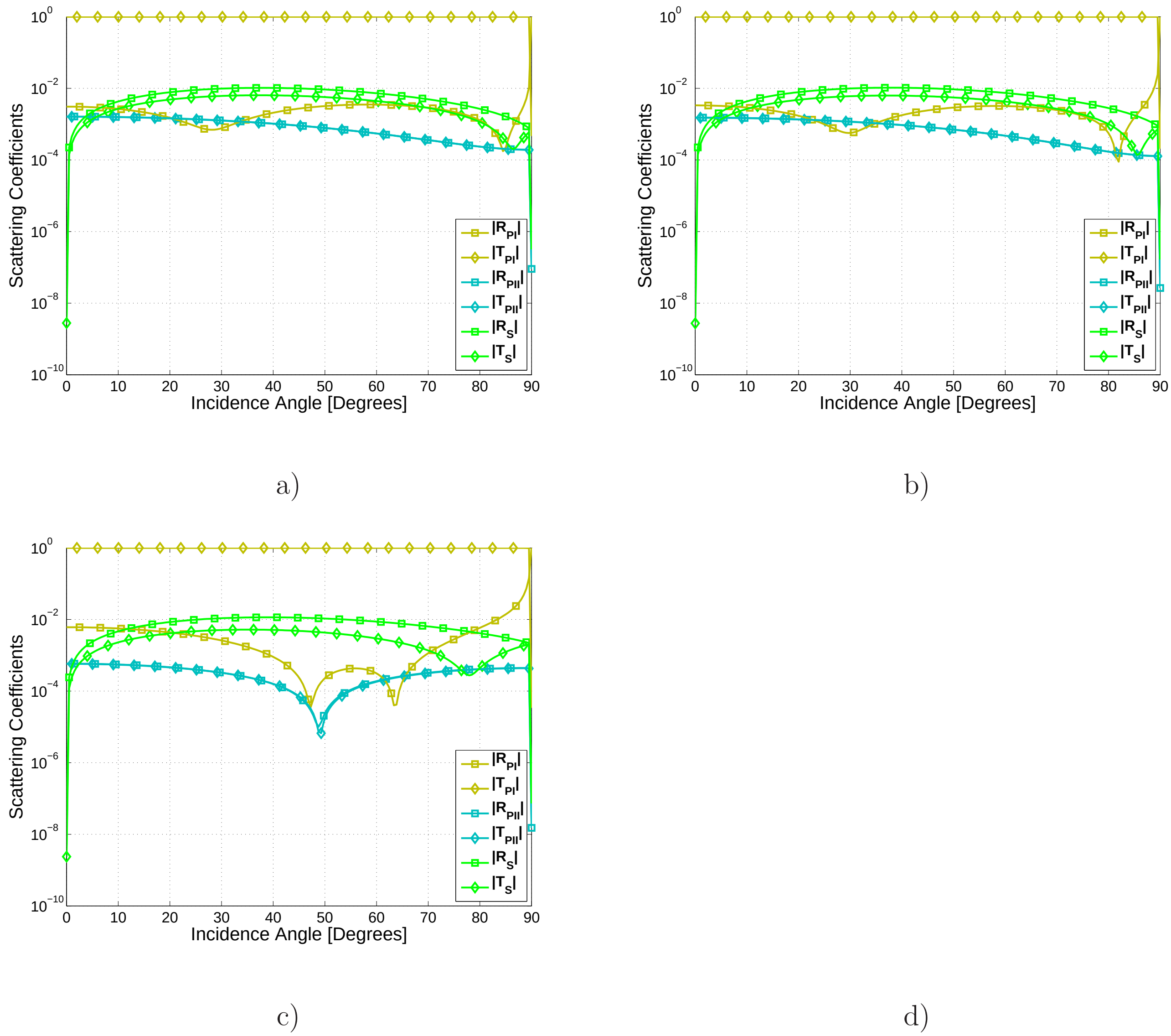

Figure 6: Reflection and transmission coefficients of type I (PI), type II (PII) and shear waves as a function of the incidence angle. The coefficients were calculated using Equation 52 of (31). The incident wave is a type I P-wave of frequency 50 Hz, permeability $\kappa_0 = 100$ D and h =0.001 m. a) Water in the fracture; b) oil in the fracture; c) gas in the fracture.